

Analysis of the fusion excitation functions for the $^{28}\text{Si} + ^{94,100}\text{Mo}$ systems

M. Ramezani* and O. N. Ghodsi

Department of Physics, Sciences Faculty, University of Mazandaran, P.O. Box 47415-416, Babolsar, Iran

(Received 22 April 2013; revised manuscript received 20 January 2014; published 28 March 2014)

This paper shows the importance of the incompressibility of nuclear matter on analyzing the fusion excitation functions, average angular momenta, and astrophysical S factor at energies far below the Coulomb barrier for the asymmetric systems $^{28}\text{Si} + ^{94}\text{Mo}$ and $^{28}\text{Si} + ^{100}\text{Mo}$. Moreover, our predictions for threshold energy of fall-off phenomena, E_s , are in good agreement with semi-empirical formulas of E_s for $^{28}\text{Si} + ^{94,100}\text{Mo}$ systems.

DOI: [10.1103/PhysRevC.89.034006](https://doi.org/10.1103/PhysRevC.89.034006)

PACS number(s): 25.70.Jj, 21.65.Mn

I. INTRODUCTION

The investigation of fusion cross sections at energies far below the Coulomb barrier has been an interesting subject in nuclear physics in recent years. Studies performed on different systems [1–9] have illustrated steep fall-off phenomena in some of the experimental data of fusion cross sections. So far, different theoretical methods, such as the double-folding (DF) model and the quantum diffusion approach, have been employed to explain these phenomena [10–13]. One mathematical tool for predicting fall-off phenomena in the fusion process is the astrophysical S factor,

$$S(E) = E\sigma(E)\exp(2\pi\eta), \quad (1)$$

where E is the center-of-mass energy, $\eta = (Z_1 Z_2 e^2)/(\hbar V_{\text{rel}})$ is the Sommerfeld parameter, and V_{rel} is the relative velocity of the target and projectile nuclei. It has been shown that by using this factor one can estimate the occurrence energy of the fall-off phenomena. This energy can be evaluated by the semi-empirical formula

$$E_s = 0.356 \left[Z_1 Z_2 \sqrt{\frac{A_1 A_2}{A_1 + A_2}} \right]^{\frac{2}{3}}. \quad (2)$$

In this energy, the value of the S factor is maximum. In other words, when there is a maximum in the values of the S factor, one can expect the existence of fall-off phenomena in the fusion process [9]. Some theoretical studies have revealed that nuclear potentials such as Akyüz-Winther (AW) and including the intrinsic effect of colliding nuclei using the couple-channels (C.C.) formalism cannot alone explain this phenomenon in the cross section at deep sub-barrier energies. In a recent study, it was shown that by including the effect of nuclear matter incompressibility on the calculation of the nuclear part of total potential, one can explain the discrepancies between theoretical prediction of cross sections and experimental data.

In a study performed on a $^{28}\text{Si} + ^{100}\text{Mo}$ system, a slope change in the values of the S factor was reported in the measured values of this quantity [2]. Therefore, in this work, the effect of nuclear matter incompressibility on this asymmetric fusing system was investigated. In addition, this effect was also studied on a $^{28}\text{Si} + ^{94}\text{Mo}$ system.

II. THEORETICAL METHOD

We employed the AW and double-folding (DF) potentials [14,15] to calculate the nuclear part of the total potential. The AW model is a phenomenological theoretical model which is parametrized based on the Woods-Saxon potential; namely,

$$U_N^{\text{AW}}(r) = -\frac{V_o}{1 + \exp[(r - R_o)/a]}. \quad (3)$$

Here the V_o , R_o , and a parameters are defined as

$$V_o = 16\pi \frac{R_1 R_2}{R_1 + R_2} \gamma a. \quad (4)$$

$$R_o = R_1 + R_2, \quad (5)$$

and

$$a = \left[\frac{1}{1.17[1 + 0.53(A_1^{-1/3} + A_2^{-1/3})]} \right]. \quad (6)$$

The R_i and γ parameters in Eqs. (4) and (5), respectively, stand for the radius of the target and of the projectile. The surface energy coefficient can be written as

$$R_i = 1.2A_i^{-1/3} - 0.09 \quad (i = 1, 2), \quad (7)$$

$$\gamma = \gamma_o \left[1 - \kappa_s \left(\frac{N_p - Z_p}{A_p} \right) \left(\frac{N_t - Z_t}{A_t} \right) \right], \quad (8)$$

where $\gamma_o = 0.95$ (MeV/fm²) and $\kappa_s = 1.8$; also $A_{p(t)}$, $Z_{p(t)}$, and $N_{p(t)}$ are characteristics of the target and projectile.

The interaction between two ions in the DF model can be evaluated by double-folding integrals,

$$U_{\text{DF}}(\mathbf{R}) = \int d\mathbf{r}_1 \int d\mathbf{r}_2 \rho_1(\mathbf{r}_1) \rho_2(\mathbf{r}_2) v_{NN}(\mathbf{r}_{12}), \quad (9)$$

where v_{NN} is the nucleon-nucleon force (NN) and $\mathbf{r}_{12} = \mathbf{R} + \mathbf{r}_2 - \mathbf{r}_1$ is the distance between the interacting nucleons, and \mathbf{R} stands for the distance between the centers of the target and projectile nuclei. We have employed the M3Y type of NN force with a zero-range exchange part to calculate the nuclear potential. In this calculation, the nuclear density distribution function of interacting nuclei is taken as the two-parameter Fermi (2PF) profile,

$$\rho_{2\text{PF}}(r) = \frac{\rho_0}{1 + \exp[(r - R_0)/a_0]}. \quad (10)$$

*morteza_amezani@stu.umz.ac.ir

TABLE I. Radius R_0 and diffuseness a_0 parameters of ^{28}Si , ^{94}Mo [16], and ^{100}Mo [10].

Nucleus	R_0 (fm)	a_0 (fm)
^{28}Si	3.14	0.537
^{94}Mo	5.049	0.528
^{100}Mo	5.116	0.497

The ^{28}Si and ^{100}Mo nuclei are deformed in their ground states. For simplification, we have considered an effective spherical shape for the nuclear matter density of these interacting nuclei. The radius R_0 and diffuseness a_0 parameters of the chosen nuclei were taken from Refs. [10,16] and are listed in Table I.

One property of nuclear matter which is important in the calculation of nuclear potential is the incompressibility of nuclear matter. This effect could deform the tail of the potential and further alter the coefficient of diffuseness in this potential [11,17]. This effect can be simulated in calculating the DF model by adding a repulsive core interaction to the NN force [10–13,18]. This repulsive part of the nuclear potential can be calculated by

$$U_{\text{rep}}(\mathbf{R}) = \int d\mathbf{r}_1 \int d\mathbf{r}_2 \rho_1(\mathbf{r}_1) \rho_2(\mathbf{r}_2) v_{\text{rep}}(\mathbf{r}_{12}), \quad (11)$$

where $v_{\text{rep}} = V_{\text{rep}}\delta(r_{12})$ and V_{rep} are adjustable parameters.

In general, the formalism of the DF model is based on sudden approximation. In other words, in this formalism it is assumed that the fusion reaction happens so fast that the nuclear matter density of each one of the interacting nuclei has no chance to change its shape during the fusion process. Based on this approximation, the density of nuclear matter in the complete overlapping region can be increased to values higher than the saturation density (i.e., $\rho_0 = 0.162 \text{ fm}^{-3}$). Nevertheless, one can expect some variation in the profiles of the nuclear matter density of interacting nuclei in this region due to the incompressibility property of nuclear matter. Therefore, in calculating the integrals of Eq. (11) the diffuseness constant for density distribution was assumed to be a_{rep} , namely,

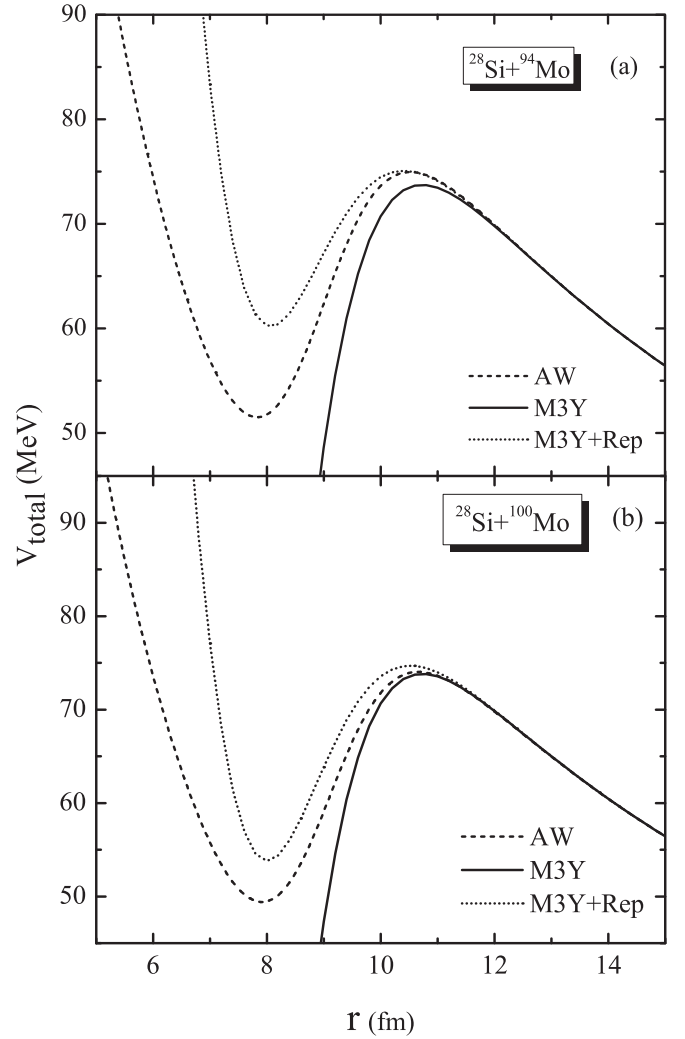
$$\rho_i(r) = \frac{\rho_0}{1 + \exp[(r - R_0)/a_{\text{rep}}]}, \quad (12)$$

and it is taken as an adjustable parameter.

One condition which can be employed to set the values of these adjustable parameters is the variation of energy when two interacting nuclei completely overlap. This variation of

TABLE II. Parameters used in calculating the repulsive, double-folding potential for two reactions, and the associated pocket energy.

Reaction	a_{rep} (fm)	V_{rep} (MeV)	V_{pocket} (MeV)
$^{28}\text{Si} + ^{94}\text{Mo}$	0.461	422.8	60.25
$^{28}\text{Si} + ^{100}\text{Mo}$	0.423	405	53.81

FIG. 1. Total interaction potential for $^{28}\text{Si} + ^{94}\text{Mo}$ and $^{28}\text{Si} + ^{100}\text{Mo}$ based on the AW, M3Y, and M3Y+Rep models.

energy can be estimated by

$$\Delta U \approx 2A_P[\varepsilon(2\rho_0, \delta) - \varepsilon(\rho_0, \delta)], \quad (13)$$

where $\varepsilon(\rho, \delta)$ is the equation state of nuclear matter, δ and ρ_0 are, respectively, the relative neutron excess and the saturation density of nuclear matter, and A_P is mass number of the projectile nucleus. We have used the Thomas-Fermi model to calculate the $\varepsilon(\rho, \delta)$ [19].

TABLE III. Properties of the 2^+ and 3^- states in the target (^{94}Mo , ^{100}Mo) and projectile (^{28}Si) nuclei [20,21].

Nucleus	λ^π	E_x (MeV)	β_λ
^{28}Si	2^+	1.779	0.407
	3^-	6.878	0.390
^{94}Mo	2^+	0.871	0.150
	3^-	2.533	0.161
^{100}Mo	2^+	0.535	0.230
	3^-	1.908	0.155

The constants a_{rep} and V_{rep} were chosen so that the calculated value of nuclear potential at $r = 0$ and the values of the fusion cross sections and average angular momenta, respectively, would be in agreement with the predicted values obtained from Eq. (13) and the corresponding experimental data for the fusion cross sections and average angular momenta.

The obtained values for a_{rep} and V_{rep} from analyzing $^{28}\text{Si} + ^{94}\text{Mo}$ and $^{28}\text{Si} + ^{100}\text{Mo}$ systems are listed in Table II. The M3Y interaction potential along with the modified potential (M3Y+Rep) and AW potentials are indicated for the $^{28}\text{Si} + ^{94}\text{Mo}$ and $^{28}\text{Si} + ^{100}\text{Mo}$ systems in Fig. 1. This figure shows that including the effect of the nuclear matter incompressibility in the calculation of nuclear potential leads to the appearance of shallow pockets in the internal part of the interaction potential.

The fusion cross sections and average angular momenta for the chosen systems were calculated using the CCFULL code, and the one-phonon excitations of the lowest 2^+ and 3^- states in the target and projectile were included in the calculation of these quantities. The values of excitation energies E_x and

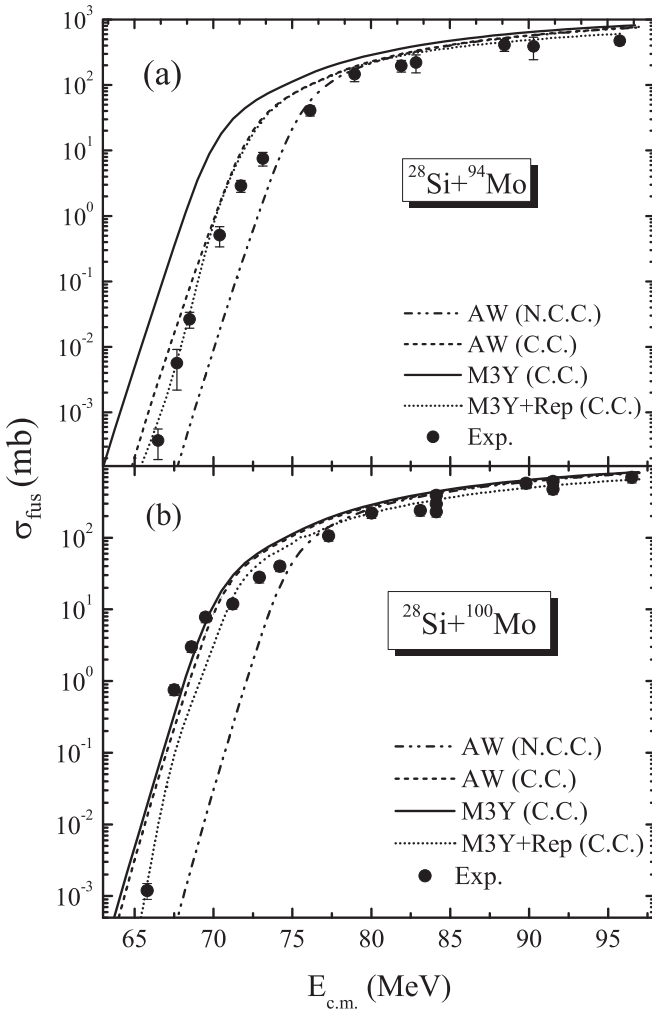


FIG. 2. Calculated fusion excitation function for systems $^{28}\text{Si} + ^{94}\text{Mo}$ and $^{28}\text{Si} + ^{100}\text{Mo}$ using AW, M3Y, and M3Y+Rep potentials. The experimental data are taken from Ref. [2].

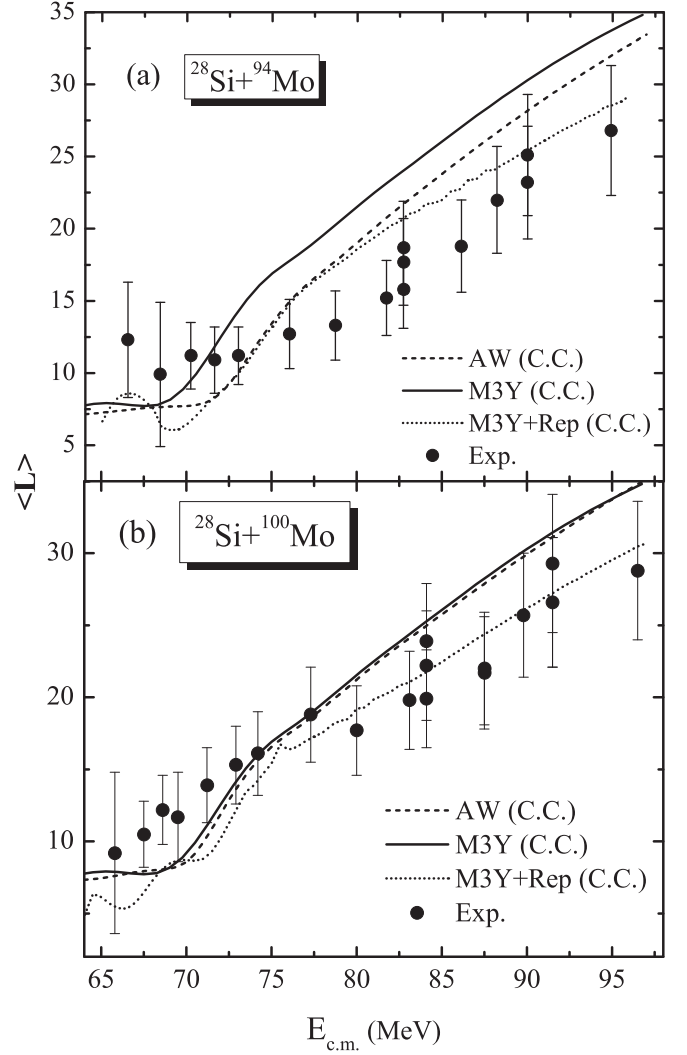


FIG. 3. Calculated angular momenta for systems $^{28}\text{Si} + ^{94}\text{Mo}$ and $^{28}\text{Si} + ^{100}\text{Mo}$ using AW, M3Y, and M3Y+Rep potentials. The experimental data are taken from Ref. [2].

deformation parameters corresponding to the excited states of interacting nuclei are listed in Table III. The calculated fusion cross sections and average angular momenta using the M3Y, M3Y+Rep, and AW potentials including the coupled-channels (C.C.) and no-coupling (N.C.C.) are compared in Figs. 2 and 3. The obtained results revealed the importance of these effects on the calculation of the fusion cross section and average angular momenta. Results were also compared with experimental data in these figures. Furthermore, the calculated values of the S factor using the M3Y, M3Y+Rep, and AW potentials are compared with the corresponding experimental data in Fig. 4 for each of these interacting systems.

III. DISCUSSION AND CONCLUSIONS

In this paper, we have analyzed the fusion excitation functions, average angular momenta, and astrophysical S factor for asymmetric systems $^{28}\text{Si} + ^{94}\text{Mo}$ and $^{28}\text{Si} + ^{100}\text{Mo}$. The fusion cross sections and average angular momenta were

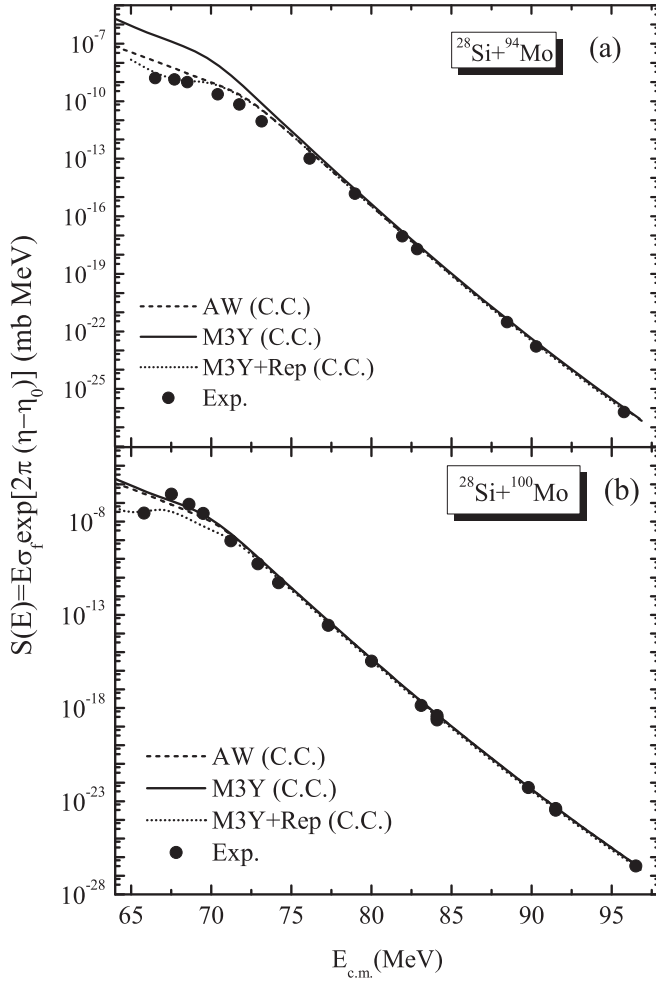


FIG. 4. Experimental S factors for the systems $^{28}\text{Si} + ^{94}\text{Mo}$ and $^{28}\text{Si} + ^{100}\text{Mo}$ compared with those obtained using the M3Y, M3Y+Rep, and AW potentials.

calculated using the AW, M3Y, and M3Y+Rep potentials. Figures 2 and 3 show that the fusion cross sections and average angular momenta calculated by the M3Y+Rep internuclear potential are in better agreement with experimental data,

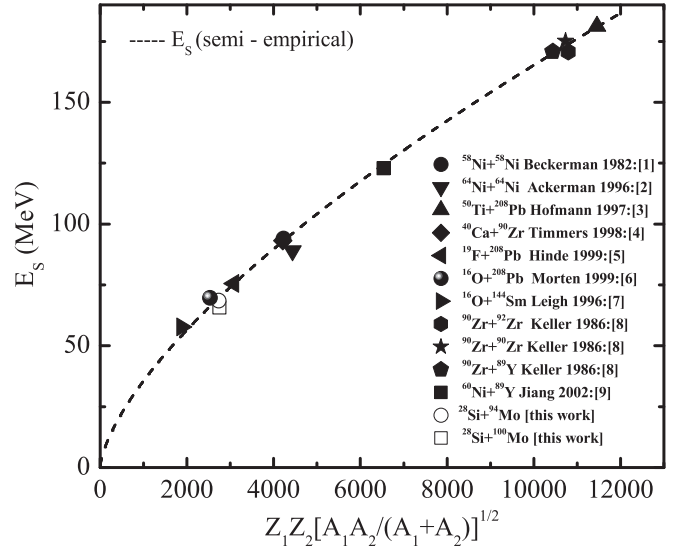


FIG. 5. Predicted values for threshold energy of fall-off phenomena compared with predictions of Eq. (2) as a function of the $Z_1 Z_2 \sqrt{\frac{A_1 A_2}{A_1 + A_2}}$ parameter. The previously obtained results for other systems [1–9] are indicated by solid symbols.

particularly at deep sub-barrier energies, than those extracted by AW and M3Y potentials. This analysis revealed that the incompressibility of nuclear matter can be important in the fusion process of these systems.

In Fig. 4, the astrophysical S factors for these systems are calculated theoretically and compared with experimental data. A slope change in the values of the S factor can be observed in this figure for $^{28}\text{Si} + ^{94}\text{Mo}$ and $^{28}\text{Si} + ^{100}\text{Mo}$ systems, respectively, in energies of 68.5 and 65.5 MeV. These energies can be the threshold energy for fall-off phenomena. These values are compared with the predictions of Eq. (2) for E_s in Fig. 5. This figure shows that there is good agreement between the prediction of this semi-empirical formula for threshold energy for the fall-off phenomenon and those we obtained theoretically for these systems. In addition, previous results obtained for other systems are indicated in this figure by the solid symbols.

- [1] M. Beckerman *et al.*, *Phys. Rev. C* **23**, 1581 (1981).
- [2] D. Ackermann, P. Bednarczyk, L. Corradi, D. R. Napoli, C. M. Petrache, P. Spolaore, A. M. Stefanini, K. M. Varier, H. Zhang, E. Scarlassara, S. Beghini, G. Montagnoli, L. Müller, G. F. Segato, F. Soramel, and C. Signorini, *Nucl. Phys. A* **609**, 91 (1996).
- [3] S. Hofmann *et al.*, *Z. Phys. A* **358**, 377 (1997).
- [4] H. Timmers *et al.*, *Nucl. Phys. A* **633**, 421 (1998).
- [5] D. J. Hinde, A. C. Berriman, M. Dasgupta, J. R. Leigh, J. C. Mein, C. R. Morton, and J. O. Newton, *Phys. Rev. C* **60**, 054602 (1999).
- [6] C. R. Morton, A. C. Berriman, M. Dasgupta, D. J. Hinde, J. O. Newton, K. Hagino, and I. J. Thompson, *Phys. Rev. C* **60**, 044608 (1999).
- [7] J. R. Leigh, M. Dasgupta, D. J. Hinde, J. C. Mein, C. R. Morton, R. C. Lemmon, J. P. Lestone, J. O. Newton, H. Timmers, J. X. Wei, and N. Rowley, *Phys. Rev. C* **52**, 3151 (1995); H. Esbensen and B. B. Back, *ibid.* **54**, 3109 (1996).
- [8] J. G. Keller *et al.*, *Nucl. Phys. A* **452**, 173 (1986).
- [9] C. L. Jiang, H. Esbensen, K. E. Rehm, B. B. Back, R. V. F. Janssens, J. A. Caggiano, P. Collon, J. Greene, A. M. Heinz, D. J. Henderson, I. Nishinaka, T. O. Pennington, and D. Seweryniak, *Phys. Rev. Lett.* **89**, 052701 (2002).
- [10] S. Misicu and H. Esbensen, *Phys. Rev. C* **75**, 034606 (2007).
- [11] H. Esbensen, C. L. Jiang, and A. M. Stefanini, *Phys. Rev. C* **82**, 054621 (2010).
- [12] V. V. Sargsyan, G. G. Adamian, N. V. Antonenko, W. Scheid, and H. Q. Zhang, *Phys. Rev. C* **86**, 034614 (2012).

- [13] R. A. Kuzyakin, V. V. Sargsyan, G. G. Adamian, N. V. Antonenko, E. E. Saperstein, and S. V. Tolokonnikov, [Phys. Rev. C **85**, 034612 \(2012\)](#).
- [14] A. Winther, [Nucl. Phys. A **594**, 203 \(1995\)](#).
- [15] G. R. Satchler and W. G. Love, [Phys. Rep. **55**, 183 \(1979\)](#).
- [16] H. De Vries, C. W. De Jager, and C. Dr Vries, [At. Data Nucl. Data Tables **36**, 495 \(1987\)](#).
- [17] O. N. Ghodsi and V. Zanganeh, [Nucl. Phys. A **846**, 40 \(2010\)](#).
- [18] E. Uegaki and Y. Abe, [Prog. Theor. Phys. **90**, 615 \(1993\)](#).
- [19] W. D. Myers and W. J. Swiateki, [Phys. Rev. C **57**, 3020 \(1998\)](#).
- [20] S. Raman, C. W. Nestor, Jr., and P. Tikkanen, [At. Data Nucl. Data Tables **78**, 1 \(2001\)](#).
- [21] T. Kibédi and R. H. Spear, [At. Data Nucl. Data Tables **80**, 35 \(2002\)](#).